

Spatiotemporal dynamics of a diffusive consumer-resource model with explicit spatial memory

Yongli Song¹ | Junping Shi²  | Hao Wang³ 

¹ School of Mathematics, Hangzhou Normal University, Hangzhou, China

² Department of Mathematics, William & Mary, Williamsburg, Virginia, USA

³ Department of Mathematical and Statistical Sciences, University of Alberta, Edmonton, Canada

Correspondence

Hao Wang, Department of Mathematical and Statistical Sciences, University of Alberta, Edmonton, AB T6G 2G1, Canada.
Email: hao8@ualberta.ca

Funding information

Natural Sciences and Engineering Research Council of Canada; National Natural Science Foundation of China; National Science Foundation of United States; Zhejiang Provincial Natural Science Foundation of China

Abstract

Spatial memory is inevitable in animal movement modeling but elusive in many classical models. A nonlocal integral term involving space is a traditional way to incorporate spatial memory, but the actual spatial memory should depend on past information so that delay naturally arises. We propose a new consumer-resource model with random and memory-based diffusions in which the resource species has no memory or cognition, whereas the consumer species has spatial memory. By using the memory-based diffusion coefficient and the averaged memory period of the consumer as the control parameters, we find Hopf bifurcations and stability switches occur and spatially nonhomogeneous periodic solutions are generated. It is well known that prey-taxis enhances the stability of a homogeneous coexistence state in a predator-prey system, and here we show that memory-based prey-taxis can destabilize a constant coexistence and generate complex spatiotemporal pattern formation. Using the obtained theoretical results,

we study the impact of the memory-based diffusion on the consumer-resource dynamics with Holling type-I and type-II functional responses.

KEYWORDS

consumer-resource, delay, diffusion, Hopf bifurcation, spatial memory, stability

JEL CLASSIFICATION

35B10, 35B32, 35K57, 37G05, 92B05

1 | INTRODUCTION

The mechanistic modeling of animal movements has been a hot topic for several decades. The significance of incorporating spatial memory and cognition into the modeling of animal movements has been pointed out in the review paper,¹ and the mechanistic modeling of memory and learning in animal movements has been thoroughly discussed in the synthesis paper.² For example, blue whales seem to follow the past long-term distribution of chlorophyll-a in the ocean; thus, explicit spatial memory is a necessary component in modeling blue whale movement and for predicting blue whale migrations under global climate change.^{3,4} However, spatial memory is complicated and poorly understood in both empirical and theoretical studies. Our recent spatial memory modeling paper⁵ integrated spatial cognition and memory into a classical single species model with diffusive movement in the simplest and self-contained way via a modified Fick's law. The main characteristic of the model proposed in Ref. 5 is that a discrete delay (known as memory delay) is involved in the diffusion term. Note that spatial memory naturally depends on past information so that delay should be explicitly incorporated. Recently, there has been an increasing activity and interest on the dynamics of the single population model with memory-based diffusion.⁶⁻¹⁰ It has been shown in Ref. 5 that the stability of a spatially homogeneous steady state fully depends on the reaction term and the ratio of the two diffusion coefficients but is independent of the memory delay, whereas the cooperation of both memory delay and maturation delay can affect the stability of a spatially homogeneous steady state.⁷ In Refs. 6 and 9, to incorporate spatial memory and non-local effect of animal movements with or without a maturation delay, we propose and investigate the spatiotemporal dynamics of the single population model with memory-based diffusion and nonlocal reaction. In Refs. 8 and 10, the influence of the spatiotemporal distributed delays on the stability of the spatially homogeneous steady state is investigated.

In this paper, we extend the single species model with spatial memory to a consumer-resource model with spatial memory of the consumer. Fagan et al proposed an advection-diffusion consumer-resource model with an integral function for consumer's resource perception.¹¹ Their resource-based advection term has the same structure as our memory-based diffusion term derived in Ref. 5: The advection velocity in Ref. 11 is the gradient of resource, and the advection velocity in Ref. 5 is the gradient of past animal density. The assumption "the higher animal density leads to the lower resource density" gives the opposite signs in the beginning of these two terms. The model in Ref. 11 has the consumer's cognition but no spatial memory, whereas our model in this paper has spatial memory explicitly. In addition, the model in Ref. 11 has static resource with distribution determined by landscape, whereas our model has dynamic resource. We can have

landscape-dependent parameters in the resource equation, which may be more realistic in many situations. For simplicity, we assume that landscape is spatially homogeneous in this paper.

We consider the prey–predator interaction (u -density of prey, v -density of predator) with their movements. The movements include both random walk and spatial memory-based walk. The random walk, expressed as diffusion equation, is based on the basic mass balance law and the Fick’s law, which assumes that the movement flux is in the direction of negative gradient of the density distribution function, that is,

$$\begin{cases} \mathbf{J}_u(x, t) = -d_{11} \nabla u(x, t), \\ \mathbf{J}_v(x, t) = -d_{22} \nabla v(x, t). \end{cases} \tag{1}$$

To incorporate the spatial memory-based walk, we assume that the prey (or the predator) makes the memory-based decision according to the predator (or the prey) distribution they remember. Here, we assume that their own memorized distributions are negligible compared to the predation thread (or the prey availability). We propose a modified Fick’s law that in addition to the negative gradient of the density distribution function at the present time, there is a directed movement of the prey (or the predator) toward the negative (or positive) gradient of the predator (or the prey) density distribution function at a *past time*. This suggests a flux in the form of

$$\begin{cases} \mathbf{J}_u(x, t) = -d_{11} \nabla u(x, t) - d_{12} u(x, t) F(\nabla v(x, t - \tau_1)), \\ \mathbf{J}_v(x, t) = -d_{22} \nabla v(x, t) + d_{21} v(x, t) G(\nabla u(x, t - \tau_2)), \end{cases} \tag{2}$$

where d_{11} and d_{22} are the Fickian diffusion coefficients, d_{12} and d_{21} are the memory-based diffusion coefficients, the time delays $\tau_i > 0$ ($i = 1, 2$) represent the averaged memory periods of prey and predator, and F and G are functions showing the dependence of memory-based diffusion on the opponent population gradients at τ_i ($i = 1, 2$) time units before the present time. The memory-based diffusion flux is proportional to the population density at present time and the opponent spatial gradients at a past time. By using the modified Fick’s law in (2) and combining the chemical/biological processes of the species, the density functions $u(x, t)$ and $v(x, t)$ satisfy the following reaction–diffusion equations:

$$\begin{cases} \frac{\partial u}{\partial t}(x, t) = d_{11} \Delta u(x, t) + d_{12} \operatorname{div}(u(x, t) F(\nabla v(x, t - \tau_1))) + f(x, t, u(x, t), v(x, t)), \\ \frac{\partial v}{\partial t}(x, t) = d_{22} \Delta v(x, t) - d_{21} \operatorname{div}(v(x, t) G(\nabla u(x, t - \tau_2))) + g(x, t, u(x, t), v(x, t)), \end{cases} \tag{3}$$

where f and g describe the chemical reaction or biological birth/death of prey and predator, and f and g are sufficient smooth if needed.

For simplicity, in the following, we assume that F and G are identity functions, and f and g follow a classical autonomous prey–predator interaction. In this paper, the prey is considered as a resource such as plants or “drunk” animals. In this scenario, the prey has no memory or cognition, that is, $d_{12} = 0$, then the consumer-resource model with random and memory-based diffusions

subject to Neumann boundary condition is as follows:

$$\left\{ \begin{array}{ll} u_t(x, t) = d_{11}\Delta u(x, t) + f(u(x, t), v(x, t)), & x \in \Omega, t > 0, \\ v_t(x, t) = d_{22}\Delta v(x, t) - d_{21}\operatorname{div}(v(x, t)\nabla u(x, t - \tau)) \\ \quad + g(u(x, t), v(x, t)), & x \in \Omega, t > 0, \\ \frac{\partial u(x, t)}{\partial \nu} = \frac{\partial v(x, t)}{\partial \nu} = 0, & x \in \partial\Omega, t > 0, \\ u(x, t) = u_0(x, t), & x \in \Omega, t \in [-\tau, 0], \\ v(x, t) = v_0(x), & x \in \Omega, \end{array} \right. \quad (4)$$

where $d_{11}, d_{22} > 0, d_{21} \geq 0, \tau = \tau_2$ (due to only one delay now), Ω is a bounded domain in \mathbb{R}^N ($N \geq 1$) with C^2 boundary $\partial\Omega$, and ν is the unit outer normal vector of the boundary $\partial\Omega$.

In general, if we consider spatially nonhomogeneous landscape and consider seasonality or sudden events, then the parameters depend on both space and time, that is, the reaction terms become $f(x, t, u(x, t), v(x, t))$ and $g(x, t, u(x, t), v(x, t))$, and the diffusion coefficients become $d_{11}(x, t), d_{21}(x, t), d_{22}(x, t)$. Here we ignore these complexities so that we can effectively perform stability and bifurcation analysis. Biologically, this is also an important and feasible start for a spatial memory-based consumer-resource model.

The model (3) is also an extension of the prey-taxis/predator-taxis reaction–diffusion model in which the prey population tries to evade the predator population while the predator population chases the prey. Indeed, the version of (3) when $\tau_1 = \tau_2 = 0$ with both prey-taxis and predator-taxis was proposed in Refs. 12 and 13, whereas the version of (4) with $\tau = 0$ with only prey-taxis was proposed and studied in Refs. 14–17, see also^{18–24} for more recent studies on global existence and boundedness of solutions and existence of nonconstant steady state or time-periodic solutions. The system with only predator-taxis was studied in Ref. 25.

Our main result in the paper is: if the prey (resource) and predator (consumer) achieves a stable homogenous coexistence state when the two species only move following passive diffusion (i.e., $d_{11}, d_{22} > 0$ and $d_{21} = 0$), then such stability remains the same with the addition of a prey-taxis with $d_{21} > 0$ (but $\tau = 0$); however, when d_{21} passes some threshold $d_{21}^* > 0$ and $\tau > \tau_*(d_{21})$, the homogenous coexistence state becomes unstable and an associated Hopf bifurcation generates a spatially nonhomogeneous time-periodic solution. That is, a memory-based predator movement toward high prey concentration (prey-taxis) leads to time-periodic motion of both prey and predator. It is well known that (memory-less) prey-taxis, in general, enhances the stability of a homogeneous coexistence state in a predator–prey system;^{13,17,22,23} however, in this paper, we show that memory-based prey-taxis destabilizes a homogeneous coexistence state and it is a new mechanism for spatiotemporal pattern formation.

The paper is organized as follows. In Section 2, we address the well-posedness of solutions to system (4). In Section 3, we investigate the distribution of characteristic roots and derive the conditions for the stability of the constant coexistence equilibrium, delay-induced Hopf bifurcations, and stability switches. In Section 4, we apply the theoretical results in Section 3 to investigate the dynamics of the consumer-resource model with Holling type-I/type-II functional response. We discuss our model and results in Section 5. Throughout the paper, \mathbb{N} represents the set of all positive integers, and $\mathbb{N}_0 = \mathbb{N} \cup \{0\}$ represents the set of all nonnegative integers.

2 | WELL-POSEDNESS OF SOLUTIONS

In this section, we investigate the well-posedness (existence, uniqueness, and positivity) of solutions to system (4) with the following assumptions on the initial condition:

$$\begin{cases} u_0(x, t) \in C^{2,\alpha}(\bar{\Omega} \times [-\tau, 0]), & \frac{\partial u_0(x,t)}{\partial \nu} = 0, (x, t) \in \partial\Omega \times [-\tau, 0], \alpha \in (0, 1), \\ v_0(x) \in C^2(\bar{\Omega}). \end{cases} \tag{5}$$

We assume that functions f, g in (4) satisfy

- (f_1) Assume that $f \in C^1([0, \infty] \times [0, \infty], \mathbb{R})$, $f(0, v) = 0$ for $v \geq 0$, and there exists $F : [0, \infty) \rightarrow \mathbb{R}$ and $M > 0$ such that $f(u, v) \leq F(u)$, and F satisfies $F(0) = 0, F(u) < 0$ for $u > M$.
- (g_1) Assume that $g \in C^1([0, \infty] \times [0, \infty], \mathbb{R})$, $g(u, 0) = 0$ for $u \geq 0$, and there exist $K_1 > 0, K_2 > 0$ such that $g(u, v) \leq (K_1 + K_2u)v$.

Proposition 1. *Suppose that $d_{11} > 0, d_{22} > 0, d_{12} \in \mathbb{R}, \tau > 0, \Omega$ is a bounded, connected open subset of \mathbb{R}^N with C^2 boundary $\partial\Omega$, and f, g satisfy (f_1) and (g_1). Then system (4) with the initial condition (5) possesses a unique solution $(u(x, t), v(x, t))$ for $(x, t) \in \bar{\Omega} \times [0, \infty)$, and $u(x, t), v(x, t) \in C^{2,1}(\bar{\Omega} \times [0, \infty))$. Moreover, if $u_0(x, t) > 0$ for $(x, t) \in \bar{\Omega} \times [-\tau, 0), v_0(x) \geq (\neq)0$ for $x \in \bar{\Omega}$, then $u(x, t) > 0, v(x, t) > 0$ for $(x, t) \in \bar{\Omega} \times [0, \infty)$.*

Proof. For $t \in [0, \tau]$, $u(x, t - \tau)$ coincides with the initial function $u_0(x, t)$. Setting

$$\begin{aligned} F^{(1)}(t, x, u, v) &= f(u(x, t), v(x, t)), \\ F^{(2)}(t, x, u, v) &= -d_{21} \operatorname{div}(v(x, t) \nabla u_0(x, t - \tau)) + g(u(x, t), v(x, t)), \end{aligned} \tag{6}$$

then it follows from (f_1) and (g_1) that $F^{(1)}$ and $F^{(2)}$ are continuous and satisfy a Hölder condition with respect to t , a Lipschitz condition with respect to u and v . As $\partial\Omega$ is C^2 , it follows from Ref. [26, Proposition 7.3.3] that $u(x, t), v(x, t)$ can be solved uniquely on $[0, \delta]$ for some $\delta > 0$. The condition (f_1) guarantees that $u(x, t)$ can be extended to $[0, \tau]$, so $u(x, t)$ is also bounded on $[0, \tau]$ by a constant $B_0 > 0$. According to (g_1), $v(x, t)$ satisfies

$$\begin{cases} v_t(x, t) \leq d_{22} \Delta v(x, t) - d_{21} \operatorname{div}(v(x, t) \nabla u_0(x, t - \tau)) + (K_1 + K_2 B_0)v, & x \in \Omega, 0 < t < \tau, \\ \frac{\partial v(x,t)}{\partial \nu} = 0, & x \in \partial\Omega, t > 0, \\ v(x, 0) = v_0(x), & x \in \Omega, \end{cases} \tag{7}$$

then $v(x, t)$ can also be extended to $[0, \tau]$. Repeating this process, the solution can be extended to $[\tau, 2\tau]$ and further to $[k\tau, (k + 1)\tau]$ for any $k \in \mathbb{N}$. Moreover, from the maximum principle, $u(x, t) > 0$ and $v(x, t) > 0$ for $(x, t) \in \bar{\Omega} \times [0, \infty)$. ■

3 | DELAY-INDUCED HOPF BIFURCATION AND STABILITY SWITCHES

In this section, we consider delay-induced instability and stability switches of a constant steady state in system (4). We assume that $E_* = (u_*, v_*)$ is a constant coexistence (positive) equilibrium of system (4). The linearization of system (4) at (u_*, v_*) is

$$\begin{pmatrix} u_t(x, t) \\ v_t(x, t) \end{pmatrix} = D_1 \begin{pmatrix} \Delta u(x, t) \\ \Delta v(x, t) \end{pmatrix} + D_2 \begin{pmatrix} \Delta u(x, t - \tau) \\ \Delta v(x, t - \tau) \end{pmatrix} + A \begin{pmatrix} u(x, t) \\ v(x, t) \end{pmatrix}, \tag{8}$$

where

$$D_1 = \begin{pmatrix} d_{11} & 0 \\ 0 & d_{22} \end{pmatrix}, \quad D_2 = \begin{pmatrix} 0 & 0 \\ -d_{21}v_* & 0 \end{pmatrix}, \quad A = \begin{pmatrix} a_{11} & a_{12} \\ a_{21} & a_{22} \end{pmatrix}, \tag{9}$$

and

$$a_{11} = \frac{\partial f(u_*, v_*)}{\partial u}, \quad a_{12} = \frac{\partial f(u_*, v_*)}{\partial v}, \quad a_{21} = \frac{\partial g(u_*, v_*)}{\partial u}, \quad a_{22} = \frac{\partial g(u_*, v_*)}{\partial v}. \tag{10}$$

Let σ_n be the eigenvalues of

$$\Delta w(x) + \sigma w(x) = 0, \quad x \in \Omega, \quad \frac{\partial w(x)}{\partial \nu} = 0, \quad x \in \partial\Omega, \tag{11}$$

satisfying $0 = \sigma_0 < \sigma_1 \leq \sigma_2 \leq \dots$, and let $w_n(x)$ be the eigenfunction corresponding to σ_n . In this paper, we assume that for $n \in \mathbb{N}$, all σ_n are simple eigenvalues with a one-dimensional eigenspace. Note that this assumption holds for generic domain Ω in \mathbb{R}^N , and it always hold for a one-dimensional domain $\Omega = (0, \ell\pi)$ with $\sigma_n = n^2/\ell^2$ and $w_n(x) = \cos(nx/\ell)$ where $\ell > 0$ is a length parameter. Assume that the solution of (8) is in form of

$$\begin{pmatrix} u_t(x, t) \\ v_t(x, t) \end{pmatrix} = \sum_{n=0}^{\infty} \begin{pmatrix} A_n \\ B_n \end{pmatrix} e^{\lambda_n t} w_n(x). \tag{12}$$

From the orthogonality of the eigenfunctions $\{w_n : n \in \mathbb{N}_0\}$, one can conclude that λ_n is the root of $\det(\mathcal{M}_n(\lambda)) = 0$ where the characteristic matrix

$$\mathcal{M}_n(\lambda) = \lambda I_2 + \sigma_n D_1 + \sigma_n e^{-\lambda\tau} D_2 - A, \tag{13}$$

and I_2 is the 2×2 identity matrix. Hence, the characteristic equation of (8) is

$$\prod_{n \in \mathbb{N}_0} \Gamma_n(\lambda) = 0, \tag{14}$$

where

$$\Gamma_n(\lambda) = \det(\mathcal{M}_n(\lambda)) = \lambda^2 - T_n \lambda + \tilde{J}_n(\tau) = 0, \tag{15}$$

and

$$\begin{aligned}
 T_n &= Tr(A) - Tr(D_1)\sigma_n, \\
 \tilde{J}_n(\tau) &= d_{11}d_{22}\sigma_n^2 - (d_{11}a_{22} + d_{22}a_{11} + d_{21}v_*a_{12}e^{-\lambda\tau})\sigma_n + Det(A),
 \end{aligned}
 \tag{16}$$

with $Tr(A) = a_{11} + a_{22}$, $Tr(D_1) = d_{11} + d_{22}$ and $Det(A) = a_{11}a_{22} - a_{12}a_{21}$.

For biological relevance of a consumer-resource model, throughout the paper, we always assume that

$$(C_0) \quad a_{12} < 0, \quad a_{21} > 0.$$

This implies that u is the prey and v is the predator in (4). We further assume that the following two conditions

$$(C_1) \quad Tr(A) < 0, \quad Det(A) > 0,$$

and

$$(C_2) \quad d_{11}a_{22} + d_{22}a_{11} < 2\sqrt{d_{11}d_{22}Det(A)}$$

hold. The condition (C_1) implies that the positive constant equilibrium E_* is locally asymptotically stable for (4) without diffusion ($d_{ij} = 0$ for $i, j = 1, 2$), and (C_2) implies that there is no diffusion-driven Turing instability for (4) with only passive diffusion but without spatial memory diffusion ($d_{21} = 0$) (see Ref. 27, Section 2.3).

Set

$$J_n = d_{11}d_{22}\sigma_n^2 - (d_{11}a_{22} + d_{22}a_{11})\sigma_n + Det(A), \tag{17}$$

It is easy to verify that under the conditions (C_1) and (C_2) ,

$$T_n < 0, \quad J_n > 0, \quad n \in \mathbb{N}_0, \tag{18}$$

which implies that when $d_{21} = 0$, the positive constant equilibrium E_* of (4) is locally asymptotically stable for any $d_{11}, d_{22} \geq 0$. Notice that

$$\tilde{J}_n(0) = J_n - d_{21}v_*a_{12}\sigma_n. \tag{19}$$

So, $J_n > 0$ implies $\tilde{J}_n(0) > 0$ since $a_{12} < 0$ and $d_{21} > 0$. Therefore, under the conditions (C_0) , (C_1) , and (C_2) , the positive equilibrium E_* is locally asymptotically stable for (4) with $d_{21} > 0$ and $\tau = 0$.

In what follows, for $d_{21} > 0$, we take τ and d_{21} as bifurcation parameters, and investigate the influence of the spatial memory-based diffusion on the stability of the positive constant equilibrium E_* . The stability of the positive constant equilibrium E_* depends on the distribution of roots of (15) for all $n \in \mathbb{N}$. In particular, we look for the conditions such that (15) has roots with zero real parts for some $n \in \mathbb{N}$, which indicates the change of stability. First, notice that under the conditions (C_0) , (C_1) , and (C_2) , we have $\Gamma_n(0) = J_n - d_{21}v_*a_{12}\sigma_n > 0$. This implies that $\lambda = 0$ is not a root of Equation (15) for any $n \in \mathbb{N}$ and there is no occurrence of steady-state bifurcations under these conditions. Thus, the instability must occur in a form of wave instability with a purely imaginary $\lambda = \pm i\omega$.

Let $\lambda = i\omega$ ($\omega > 0$) be a root of (15). Substituting it into (15) and separating the real and imaginary parts, we have

$$\begin{cases} J_n - \omega^2 = \sigma_n d_{21} v_* a_{12} \cos(\omega\tau), \\ T_n \omega = \sigma_n d_{21} v_* a_{12} \sin(\omega\tau), \end{cases} \quad (20)$$

which yields

$$\omega^4 + P_n \omega^2 + Q_n = 0, \quad (21)$$

where

$$P_n = T_n^2 - 2J_n = (d_{11}^2 + d_{22}^2)\sigma_n^2 - 2(d_{11}a_{11} + d_{22}a_{22})\sigma_n + a_{11}^2 + a_{22}^2 + 2a_{12}a_{21}, \quad (22)$$

and

$$Q_n = (J_n - d_{21}v_*a_{12}\sigma_n)(J_n + d_{21}v_*a_{12}\sigma_n). \quad (23)$$

The solvability of (21) also depends on the discriminant

$$\Delta_n = P_n^2 - 4Q_n = T_n^4 - 4T_n^2J_n + 4d_{21}^2v_*^2a_{12}^2\sigma_n^2. \quad (24)$$

The number of the positive roots of Equation (21) is determined by the signs of P_n , Q_n , and Δ_n . In what follows, we use d_{21} and τ as the parameters to investigate the number of the positive roots of Equation (21) and then determine the stability of E_* and associated bifurcations.

For fixed $n \in \mathbb{N}$, define

$$d_{21}^{(n)} = \frac{J_n}{v_*|a_{12}|\sigma_n} = \frac{1}{v_*|a_{12}|} \left(d_{11}d_{22}\sigma_n + \frac{\text{Det}(A)}{\sigma_n} - (d_{11}a_{22} + d_{22}a_{11}) \right) > 0, \quad (25)$$

and

$$d_{21}^{*(n)} = \frac{|T_n|\sqrt{4J_n - T_n^2}}{2v_*|a_{12}|\sigma_n}, \quad \text{when } 4J_n > T_n^2. \quad (26)$$

Note that $0 < d_{21}^{*(n)} \leq d_{21}^{(n)}$ as $J_n^2 - \left(\frac{|T_n|\sqrt{4J_n - T_n^2}}{2}\right)^2 = \left(J_n - \frac{1}{2}T_n^2\right)^2 \geq 0$. Then we have

$$Q_n \begin{cases} > 0, & 0 < d_{21} < d_{21}^{(n)}, \\ = 0, & d_{21} = d_{21}^{(n)}, \\ < 0, & d_{21} > d_{21}^{(n)}. \end{cases} \quad (27)$$

Similarly, $\Delta_n > 0$ for all $d_{21} \geq 0$ when $4J_n \leq T_n^2$, and when $4J_n > T_n^2$,

$$\Delta_n \begin{cases} < 0, & 0 < d_{21} < d_{21}^{*(n)}, \\ = 0, & d_{21} = d_{21}^{*(n)}, \\ > 0, & d_{21} > d_{21}^{*(n)}. \end{cases} \tag{28}$$

From (27) and (28) and noticing the fact that $4J_n > T_n^2$ provided that $P_n < 0$, we obtain the following result on the positive roots of (21) when d_{21} varies.

Proposition 2. *For fixed $n \in \mathbb{N}$, we have the following results on the distribution of the positive roots of Equation (21). Define*

$$\omega_n^\pm = \sqrt{\frac{-P_n \pm \sqrt{\Delta_n}}{2}}. \tag{29}$$

- (i) *If $P_n = T_n^2 - 2J_n \geq 0$, then Equation (21) has no positive root when $0 < d_{21} \leq d_{21}^{(n)}$ and has one positive root ω_n^+ when $d_{21} > d_{21}^{(n)}$.*
- (ii) *If $P_n = T_n^2 - 2J_n < 0$, then Equation (21) has no positive root when $0 < d_{21} < d_{21}^{*(n)}$, has two positive roots ω_n^\pm when $d_{21}^{*(n)} \leq d_{21} < d_{21}^{(n)}$, and one positive root ω_n^+ when $d_{21} \geq d_{21}^{(n)}$.*

It follows from (20) that $\sin(\omega\tau) > 0$ because $T_n < 0$, $a_{12} < 0$ and $d_{21} > 0$. Therefore, we immediately have the following proposition identifying the critical delay values where (15) has purely imaginary roots.

Proposition 3. *When the positive roots ω_n^\pm of Equation (21) defined as in (29) exist, define*

$$\tau_{n,j}^\pm = \frac{1}{\omega_n^\pm} \left\{ \arccos \left\{ \frac{J_n - (\omega_n^\pm)^2}{d_{21} v_* a_{12} \sigma_n} \right\} + 2j\pi \right\}, \quad j \in \mathbb{N}_0, \quad n \in \mathbb{N}. \tag{30}$$

Then (15) has a pair of purely imaginary roots $\pm\omega_n^+i$ at $\tau = \tau_{n,j}^+$ and $\pm\omega_n^-i$ at $\tau = \tau_{n,j}^-$, respectively.

At the critical delay values $\tau = \tau_{n,j}^\pm$, we have the following transversality condition for the eigenvalues.

Lemma 1. *Let $\lambda(\tau) = \alpha(\tau) + i\beta(\tau)$ be the pair of roots of Equation (15) near $\tau = \tau_{n,j}^\pm$ satisfying $\alpha(\tau_{n,j}^\pm) = 0$ and $\beta(\tau_{n,j}^\pm) = \omega_n^\pm$. Then $\frac{d\text{Re}(\lambda(\tau))}{d\tau} \Big|_{\tau=\tau_{n,j}^+} > 0$, and $\frac{d\text{Re}(\lambda(\tau))}{d\tau} \Big|_{\tau=\tau_{n,j}^-} < 0$.*

Proof. Differentiating Equation (15) with respect to τ and noticing that λ is a function of τ , we have

$$\left(\frac{d\lambda}{d\tau}\right)^{-1} = -\frac{(2\lambda - T_n)e^{\lambda\tau}}{\sigma_n d_{21} v_* a_{12} \lambda} - \frac{\tau}{\lambda}. \tag{31}$$

Using (20) and (29), it is not hard to show that

$$\operatorname{Re}\left(\left(\frac{d\lambda}{d\tau}\right)^{-1}\Big|_{\lambda=\omega_n^\pm i, \tau=\tau_{n,j}^\pm}\right) = \pm \frac{\sqrt{\Delta_n}}{(\sigma_n d_{21} v_* a_{12})^2} \begin{cases} > 0, & \tau = \tau_{n,j}^+, \\ < 0, & \tau = \tau_{n,j}^-. \end{cases} \tag{32}$$

This, together with the fact that

$$\frac{d\operatorname{Re}(\lambda(\tau))}{d\tau} = \operatorname{Re}\left(\frac{d\lambda}{d\tau}\right), \quad \operatorname{sgn}\left(\operatorname{Re}\left(\frac{d\lambda}{d\tau}\right)\right) = \operatorname{sgn}\left(\operatorname{Re}\left(\left(\frac{d\lambda}{d\tau}\right)^{-1}\right)\right), \tag{33}$$

completes the proof. ■

By Proposition 3 and Lemma 1, we have the following result on mode- n Hopf bifurcations occurred when a delayed memory cross-diffusion is present with $d_{21} > 0$.

Theorem 1. *Assume that the conditions (C_0) , (C_1) , and (C_2) hold, and $d_{21} > 0$.*

- (i) *If Equation (21) has no positive roots for any $n \in \mathbb{N}$, then the positive constant equilibrium E_* is locally asymptotically stable with respect to (4) for any $\tau \geq 0$.*
- (ii) *For $n \in \mathbb{N}$, if Equation (21) has one positive root ω_n^+ , then there exists one sequence of Hopf bifurcation points $\tau_{n,j}^+$ (defined as in (30)) for (4) where mode- n Hopf bifurcations occur.*
- (iii) *For $n \in \mathbb{N}$, if Equation (21) has two positive roots ω_n^\pm , then there exist two sequences of Hopf bifurcation points $\tau_{n,j}^+$ and $\tau_{n,j}^-$ (defined as in (30)) for (4) where mode- n Hopf bifurcations occur.*

Finally, we discuss for a fixed $d_{21} > 0$, at which Equation (21) has positive roots, so the sequence of mode- n Hopf bifurcations in Theorem 1 exists. This mode selection determines the spatial profile of the pattern formation at such a cross-diffusion coefficient $d_{21} > 0$. Define

$$S_p = \{n \in \mathbb{N} : P_n < 0\}, \tag{34}$$

which is independent of d_{21} , and is a finite set (possibly empty) from (22) and the fact that σ_n increases in n and $\sigma_n \rightarrow \infty$ as $n \rightarrow \infty$.

From (25), it is easy to verify that $d_{21}^{(n)}$ is decreasing for $\sigma_n < \sqrt{\frac{\operatorname{Det}(A)}{d_{11}d_{22}}}$ and is increasing for $\sigma_n > \sqrt{\frac{\operatorname{Det}(A)}{d_{11}d_{22}}}$ and $d_{21}^{(n)} \rightarrow \infty$ as $n \rightarrow \infty$. This implies that $\min_{n \notin S_p} d_{21}^{(n)}$ exists. If S_p is not empty,

then $\min_{n \in S_p} d_{21}^{*(n)} > 0$ as S_p is finite and $d_{21}^{*(n)}$ exist for $n \in S_p$. Thus, we can set

$$d_{21}^* = \begin{cases} \min \left\{ \min_{n \in S_p} d_{21}^{*(n)}, \min_{n \notin S_p} d_{21}^{(n)} \right\} > 0, & \text{when } S_p \neq \emptyset, \\ \min_{n \in \mathbb{N}} d_{21}^{(n)} > 0, & \text{when } S_p = \emptyset. \end{cases} \tag{35}$$

The following result is a direct consequence of Proposition 2 and (35).

Theorem 2. Assume that the conditions (C_0) , (C_1) , and (C_2) hold.

- (i) If $0 < d_{21} < d_{21}^*$, then the positive constant equilibrium E_* is locally asymptotically stable with respect to (4) for any $\tau \geq 0$.
- (ii) If $d_{21} > d_{21}^*$, then the positive constant equilibrium E_* is possibly unstable for some mode n and some $\tau > 0$.

For each fixed $d_{21} > d_{21}^*$, there are delay-induced Hopf bifurcations using τ as the bifurcation parameter. Specifically we have the following results.

Theorem 3. Assume that the conditions (C_0) , (C_1) , and (C_2) hold.

(I) If $S_p = \emptyset$, define

$$U^1(d_{21}) = \left\{ n \in \mathbb{N} : d_{21}^{(n)} < d_{21} \right\}, \quad \tau_*(d_{21}) = \min_{n \in U^1(d_{21})} \tau_{n,0}^+, \tag{36}$$

then when $d_{21} > d_{21}^*$, the positive constant equilibrium E_* is local asymptotically stable for $\tau < \tau_*(d_{21})$ and is unstable for $\tau > \tau_*(d_{21})$, and Hopf bifurcations occur at $\tau = \tau_{n,j}^+$ for $n \in U^1(d_{21})$.

(II) If $S_p \neq \emptyset$, set

$$d_{21}^{**} = \max_{n \in S_p} \left\{ d_{21}^{(n)} \right\}. \tag{37}$$

(i) When $d_{21} \in (d_{21}^*, d_{21}^{**})$, define

$$\begin{aligned} \tilde{U}^1(d_{21}) &= \left\{ n \in \mathbb{N} : d_{21}^{(n)} < d_{21} \right\}, \quad \tilde{U}^2(d_{21}) = \left\{ n \in S_p : d_{21}^{*(n)} < d_{21} < d_{21}^{(n)} \right\}, \\ \tau_*(d_{21}) &= \min \left\{ \min_{n \in \tilde{U}^1(d_{21})} \tau_{n,0}^+, \min_{n \in \tilde{U}^2(d_{21})} \left\{ \tau_{n,0}^+, \tau_{n,0}^- \right\} \right\}. \end{aligned} \tag{38}$$

Then the positive constant equilibrium E_* is local asymptotically stable for $\tau < \tau_*(d_{21})$ and is unstable for $\tau > \tau_*(d_{21})$, and Hopf bifurcations occur at $\tau = \tau_{n,j}^\pm$ for $n \in \tilde{U}^2(d_{21})$ and at $\tau = \tau_{n,j}^+$ for $n \in \tilde{U}^1(d_{21})$. In this case, stability switches are possible.

(ii) When $d_{21} \geq d_{21}^{**}$, define

$$U(d_{21}) = S_p \cup \left\{ n \notin S_p : d_{21}^{(n)} < d_{21} \right\}, \quad \tau_*(d_{21}) = \min_{n \in U(d_{21})} \left\{ \tau_{n,0}^+ \right\}. \tag{39}$$

Then the positive constant equilibrium E_* is local asymptotically stable for $\tau < \tau_*(d_{21})$ and is unstable for $\tau > \tau_*(d_{21})$, and Hopf bifurcations occur at $\tau = \tau_{n,j}^+$ for $n \in U(d_{21})$.

Proof.

- (I) Notice the fact that $d_{21}^{(n)} \rightarrow \infty$ as $n \rightarrow \infty$. This implies that $U^1(d_{21})$ is a finite set. Since $S_p = \emptyset$, it is easy to see that $P_n \geq 0$ and $Q_n < 0$ for $n \in U^1(d_{21})$, and $P_n \geq 0$ and $Q_n \geq 0$ for $n \notin U^1(d_{21})$. Therefore, Equation (21) has one positive root ω_n^+ only for $n \in U^1(d_{21})$, and no positive root for $n \notin U^1(d_{21})$. Then the conclusion follows from Theorem 1.
- (II) If $S_p \neq \emptyset$, for fixed $d_{21} \in (d_{21}^*, d_{21}^{**})$, there exists at least one $n \in S_p$ such that $d_{21} < d_{21}^{(n)}$. For $n \in \mathbb{N}$ such that $d_{21}^{(n)} < d_{21}$, we have $Q_n < 0$. This implies that Equation (21) has one positive root ω_n^+ for $n \in \tilde{U}^1(d_{21})$. For $n \in S_p$, we have $d_{21}^{*(n)} < d_{21}^{(n)}$. Thus, for $n \in S_p$ such that $d_{21}^{*(n)} < d_{21} < d_{21}^{(n)}$, we have $P_n < 0, Q_n > 0$ and $\Delta_n > 0$. This implies that Equation (21) has two positive roots ω_n^\pm for $n \in \tilde{U}^2(d_{21})$. In addition, notice that Equation (21) has no positive root for either $n \in S_p$ such that $d_{21} \leq d_{21}^{*(n)}$ or $n \notin S_p$ such that $d_{21} \leq d_{21}^{(n)}$. In addition, notice that $\tau_{n,0}^\pm = \min_{j \in \mathbb{N}_0} \{\tau_{n,j}^\pm\}$. Again, the conclusion follows from Theorem 1.
- (II) For fixed $d_{21} > d_{21}^{**}$ and $n \in S_p$, we have $d_{21}^{(n)} < d_{21}$ and then $Q_n < 0$. Therefore, $Q_n < 0$ for $n \in U(d_{21})$, and $P_n \geq 0, Q_n \geq 0$ for $n \notin U(d_{21})$. This implies that Equation (21) has one positive root ω_n^+ only for $n \in U(d_{21})$, and no positive root for $n \notin U(d_{21})$. Then the result follows from Theorem 1.

■

Under the conditions $(C_0), (C_1),$ and (C_2) , the positive constant equilibrium (u_*, v_*) is locally asymptotically stable (and there is associated pattern formation) for the ordinary differential equation (ODE) model ($d_{11} = d_{22} = d_{21} = 0$), the reaction–diffusion model ($d_{11}, d_{22} > 0$ and $d_{21} = 0$), and the reaction–diffusion model with prey-taxis ($d_{11}, d_{22}, d_{21} > 0$ and $\tau = 0$). Theorem 3 shows that the positive constant equilibrium (u_*, v_*) could be destabilized to produce spatially non-homogeneous time-periodic patterns if there is a delayed prey-taxis in addition to the reaction–diffusion predator–prey model ($d_{11}, d_{22}, d_{21} > 0$ and $\tau > 0$).

Remark 1.

1. When $S_p = \emptyset$, for different values d_{21}^a and d_{21}^b of d_{21} such that $d_{21}^* \leq d_{21}^a < d_{21}^b$, we have $U^1(d_{21}^a) \subseteq U^1(d_{21}^b)$. This means when d_{21} increases, the number of Fourier modes of possible Hopf bifurcation increases. The most likely mode for spatial pattern when $d_{21} \approx d_{21}^*$ is n_1 such that σ_n is the closest to $\sqrt{\frac{Det(A)}{d_{11}d_{22}}}$. For the one-dimensional spatial domain $\Omega = (0, \ell\pi)$, we have

$$n_1 = \begin{cases} \tilde{n} & d_{21}^{(\tilde{n})} < d_{21}^{(\tilde{n}+1)} \\ \tilde{n} + 1, & d_{21}^{(\tilde{n})} > d_{21}^{(\tilde{n}+1)}, \end{cases} \quad \tilde{n} = \left\lceil \ell \sqrt[4]{\frac{Det(A)}{d_{11}d_{22}}} \right\rceil, \tag{40}$$

where $\lceil \cdot \rceil$ is the integer part function.

2. If the conditions (C_0) and (C_1) are satisfied but the condition (C_2) is not satisfied, then it is possible to choose $d_{11}, d_{22} > 0$ such that the positive constant equilibrium (u_*, v_*) is unstable with respect to the corresponding reaction–diffusion model, so the Turing instability occurs. It is known that a prey-taxis without delay ($d_{11}, d_{22}, d_{21} > 0$ and $\tau = 0$) can stabilize the constant equilibrium (u_*, v_*) ¹³ by setting d_{21} large. By using the similar methods in this section, we can show that the constant equilibrium (u_*, v_*) can be destabilized with a large $\tau > 0$.

By Theorem 3, the occurrence of delay-induced stability switches depends on whether the set S_p is empty or not. The following proposition gives a sufficient condition on whether S_p is empty or not, which is useful for applications to consumer-resource models.

Proposition 4. *Assume that the condition (C_1) holds, $d_{11} \leq d_{22}$ and $a_{22} \leq 0$.*

- (i) *If $a_{11}^2 + a_{22}^2 + 2a_{12}a_{21} \geq 0$, then $S_p = \emptyset$.*
- (ii) *If $a_{11}^2 + a_{22}^2 + 2a_{12}a_{21} < 0$, then there exists a positive integer $n_* \in \mathbb{N}$ such that $P_n \geq 0$ for $n \geq n_*$ and $P_n < 0$ for $n < n_*$, and then $S_p = \emptyset$ when $n_* = 1$ and $S_p = \{1, \dots, n_* - 1\}$ when $n_* \geq 2$.*

Proof. From (16) and (17), we have

$$P_n = T_n^2 - 2J_n = (d_{11}^2 + d_{22}^2)\sigma_n^2 - 2(d_{11}a_{11} + d_{22}a_{22})\sigma_n + a_{11}^2 + a_{22}^2 + 2a_{12}a_{21}. \tag{41}$$

With $T_0 < 0$ and $d_{11} \leq d_{22}$, it is easy to verify that $d_{11}a_{11} + d_{22}a_{22} < 0$ because $a_{22} \leq 0$. Therefore, $P_n > 0$ for any $n \in \mathbb{N}$ if $a_{11}^2 + a_{22}^2 + 2a_{12}a_{21} \geq 0$. This proves (i). On the other hand, if $a_{11}^2 + a_{22}^2 + 2a_{12}a_{21} < 0$, we have $P_0 < 0$ and P_n is increasing in n , which implies (ii). ■

4 | EXAMPLES

In this section, we apply the theoretical results in Section 3 to the consumer-resource models with Holling type-I or type-II functional responses and investigate possible pattern formations induced by the memory diffusion. Throughout this section, we restrict the spatial domain Ω to be the one-dimensional spatial domain $(0, \ell\pi)$ and choose $\ell = 2$ for the numerical simulations. In this case, we have $\sigma_n = (n/\ell)^2$ for $n \in \mathbb{N}_0$. In the following numerical simulations, we always choose the initial function $u(x, t) = u(x, 0)$ for $t \in [-\tau, 0]$, and for simplification of notations, we use the initial function $u(x, 0)$ instead of $u(x, t)$ for $-\tau \leq t \leq 0$.

4.1 | Holling type-I functional response

In this subsection, we consider the following consumer-resource model with Holling type-I functional response (Lotka–Volterra model):

$$\begin{cases} u_t(x, t) = d_{11}u_{xx}(x, t) + u\left(1 - \frac{u}{a}\right) - buv, & 0 < x < \ell\pi, t > 0, \\ v_t(x, t) = d_{22}v_{xx}(x, t) - d_{21}(v(x, t)u_x(x, t - \tau))_x - cv + buv, & 0 < x < \ell\pi, t > 0, \\ u_x(0, t) = u_x(\ell\pi, t) = v_x(0, t) = v_x(\ell\pi, t) = 0, & t \geq 0. \end{cases} \tag{42}$$

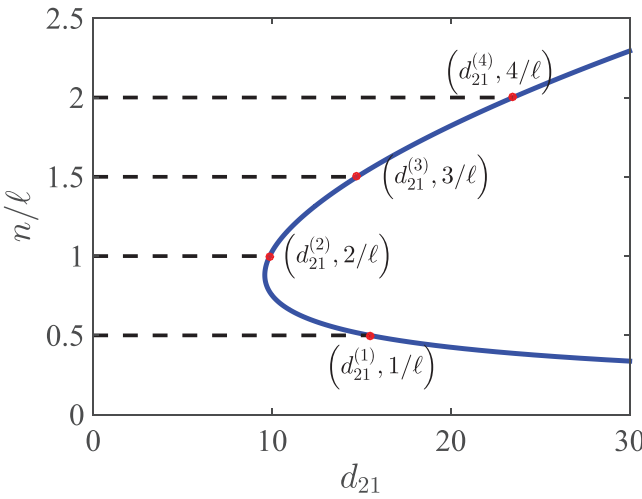


FIGURE 1 The critical values $d_{21}^{(n)}$ with respect to the wave number n for system (42) with parameters in (45). At $d_{21} = d_{21}^{(n)}, Q_n = 0$

System (42) has a unique positive equilibrium $E_* = (\frac{c}{b}, \frac{ab-c}{ab^2})$, provided that $ab > c$. For this equilibrium E_* , we have

$$a_{11} = -\frac{c}{ab} < 0, \quad a_{12} = -c < 0, \quad a_{21} = \frac{ab-c}{ab} > 0, \quad a_{22} = 0, \tag{43}$$

and

$$a_{11}^2 + a_{22}^2 + 2a_{12}a_{21} \begin{cases} \geq 0, & c \geq \frac{2a^2b^2}{1+2ab}, \\ < 0, & c < \frac{2a^2b^2}{1+2ab}. \end{cases} \tag{44}$$

From (43), we can see that the conditions (C_0) , (C_1) , and (C_2) hold. Thus, when $d_{21} = 0$, the positive equilibrium E_* is linearly stable for any $d_{11}, d_{22} > 0$. Indeed, it is well known that E_* is globally asymptotically stable for all positive initial conditions in this case.

From Proposition 4, Theorem 3, and (44), delay-induced instability and stability switches may occur only when $c < \frac{2a^2b^2}{1+2ab}$. Here we use

$$a = 2, \quad b = 3.2, \quad c = 1.6, \quad d_{11} = 1, \quad d_{22} = 2, \quad \ell = 2. \tag{45}$$

In this case, the positive constant equilibrium is $E_*(0.5, 0.2344)$ and $a_{11}^2 + a_{22}^2 + 2a_{12}a_{21} = -2.3375 < 0$. We also have $P_n = 5(n/\ell)^4 + \frac{1}{2}(n/\ell)^2 - \frac{187}{80}$, and $n^* = 2$ and $S_P = \{1\}$ for $\ell = 2$.

By (25), we can obtain the critical values $d_{21}^{(n)}$ as follows:

$$d_{21}^{(2)} \doteq 9.8667 < d_{21}^{(3)} \doteq 14.7556 < d_{21}^{(1)} \doteq 15.4667 < d_{21}^{(4)} \doteq 23.4667 < \dots \tag{46}$$

Figure 1 shows the critical values for $0 < d_{21} < 30$, and we observe that $d_{21}^{(2)}$ is the minimum of $d_{21}^{(n)}$ for $n \in \mathbb{N}$. As $n_* = 2$ and $S_P = \{1\}$, it follows from (26) and (46) that

$$\min_{n \in S_P} d_{21}^{*(n)} = d_{21}^{*(1)} \doteq 11.6847, \quad \min_{n \notin S_P} d_{21}^{(n)} = d_{21}^{(2)} \doteq 9.8667, \tag{47}$$

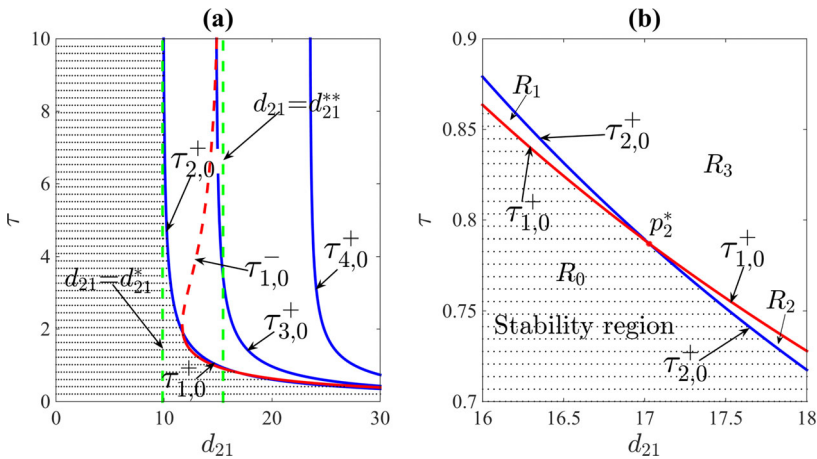


FIGURE 2 (A) Stability region and Hopf bifurcation curves in the d_{21} - τ plane for system (42) with parameters in (45). Here the blue curves are the Hopf bifurcation curves $\tau = \tau_{n,0}^+$ with $n = 2, 3, 4$, and the red curves are $\tau = \tau_{1,0}^+$; $d_{21} = d_{21}^*$ is vertical asymptotic line of $\tau = \tau_{2,j}^+$, and $d_{21} = d_{21}^{**}$ is the vertical asymptotic line of the $\tau = \tau_{1,j}^-$. (B) Enlarged (A) restricted to the region $16 \leq d_{21} \leq 18, 0.7 \leq \tau \leq 0.9$. $\tau = \tau_{2,0}^+$, and $\tau = \tau_{1,0}^+$ are Hopf bifurcation curves and p_2^* is the double Hopf bifurcation point

which, together with (35), implies that

$$d_{21}^* = \min \left\{ \min_{n \in S_p} d_{21}^{*(n)}, \min_{n \notin S_p} d_{21}^{(n)} \right\} = d_{21}^{(2)} \doteq 9.8667. \quad (48)$$

By (37), we have

$$d_{21}^{**} = \max_{n \in S_p} d_{21}^{(n)} = d_{21}^{(1)} = 15.4667, \quad (49)$$

which, together with (24), (27), and (29), implies that $\omega_1^- = 0$ for $d_{21} = d_{21}^{**}$. Thus, the straight line $d_{21} = d_{21}^{**}$ is the of the vertical asymptotic line of the Hopf bifurcation curves $\tau = \tau_{1,j}^-$.

Figure 2(A) shows the stability region and Hopf bifurcation curves associated with E_* in the d_{21} - τ plane. The dotted region is the stability region where E_* is locally asymptotically stable, and $\tau = \tau_{n,0}^\pm$ are the Hopf bifurcation curves for the positive equilibrium E_* . The boundaries of the stability region consist of the Hopf bifurcation curves $\tau = \tau_{2,0}^+$ and $\tau = \tau_{1,0}^+$. When $0 < d_{21} < d_{21}^* \doteq 9.8667$, the positive equilibrium E_* is locally asymptotically stable for any $\tau \geq 0$, and when $d_{21} > d_{21}^*$, there exists a critical delay value $\tau_*(d_{21})$ as in Theorem 3 such that the positive equilibrium E_* is locally asymptotically stable for $\tau < \tau_*$ and is unstable for $\tau > \tau_*$. There is no delay-induced stability switches for these parameters. The Hopf bifurcation curves $\tau = \tau_{2,0}^+$ and $\tau = \tau_{1,0}^+$ intersect at the points $p_1^*(11.7441, 1.9002)$ and $p_2^*(17.0276, 0.7872)$ that are double Hopf bifurcation points. Figure 2(B) is a close-up look of Figure 2(A) near the double Hopf bifurcation point p_2^* .

Guided by the bifurcation diagram in Figure 2(A), we show some numerical simulations for system (42) with parameters in (45) with $d_{21} = 10.5 \in (d_{21}^*, d_{21}^{(1)})$. In this case, we have the first Hopf bifurcation value $\tau_{2,0}^+ \doteq 3.5807$. The positive equilibrium $E_*(0.5, 0.2344)$ is asymptotically stable for $\tau < \tau_{2,0}^+ \doteq 3.5807$ as shown in Figures 3(A) and (C), and it is unstable for $\tau > \tau_{2,0}^+ \doteq 3.5807$ as shown in Figures 3(B) and (D). System (42) undergoes a Hopf bifurcation at $\tau = \tau_{2,0}^+$.

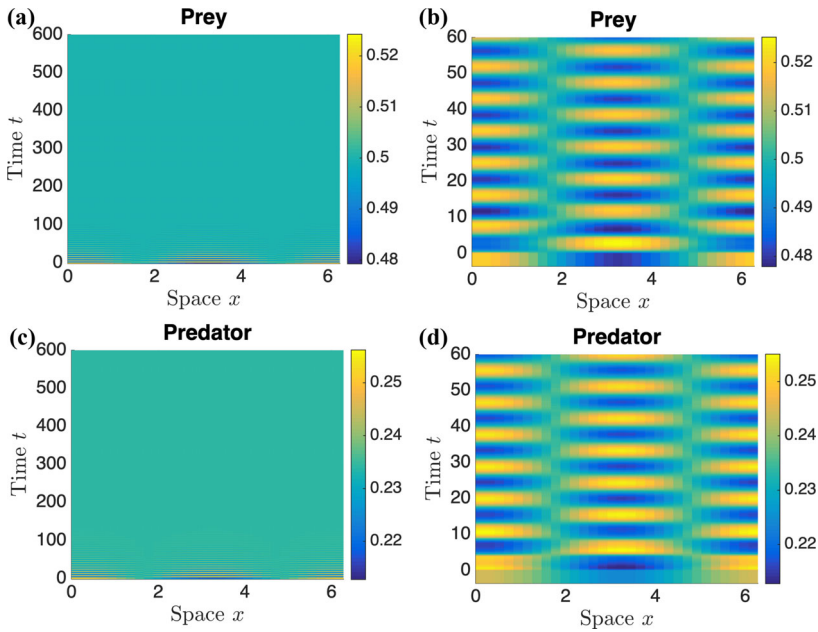


FIGURE 3 Numerical simulations for system (42) with parameters in (45) and $d_{21}^* \doteq 9.8667 < d_{21} = 10.5 < d_{21}^{*(1)} \doteq 11.6847$. (A) and (C) The positive equilibrium $E_*(0.5, 0.2344)$ is asymptotically stable for $\tau = 2 < \tau_{2,0}^+ \doteq 3.5807$. (B) and (D) The positive equilibrium $E_*(0.5, 0.2344)$ is unstable for $\tau = 3.6 > \tau_{2,0}^+ \doteq 3.5807$ and there exists a periodic solution with mode $\cos(x)$. The initial conditions are $u(x, 0) = 0.5 + 0.02 \cos(x), v(x, 0) = 0.2344 - 0.1 \cos(x)$

Figure 4 shows the numerical simulations of system (42) with parameters in (45) for (d_{21}, τ) near the double Hopf bifurcation point p_2^* in Figure 2(B). For $(d_{21}, \tau) = (16.2, 0.85) \in R_1$ in Figure 2(B), Figures 4(A) and (D) show the occurrence of a mode-1 periodic solution with spatial profile $\cos(x/2)$, which bifurcates from the Hopf bifurcation at $\tau = \tau_{1,0}^+$; for $(d_{21}, \tau) = (17.9, 0.728) \in R_2$ in Figure 2(B), Figures 4(B) and (E) show the occurrence of a mode-2 periodic solution with spatial profile $\cos(x)$, which bifurcates from the Hopf bifurcation at $\tau = \tau_{2,0}^+$. The interaction of these different mode Hopf bifurcations at $\tau = \tau_{1,0}^+$ and at $\tau = \tau_{2,0}^+$ leads to the occurrence of the quasi-periodic spatiotemporal pattern as shown in Figures 4(C) and (F) for $(d_{21}, \tau) = (17, 0.83) \in R_3$ in Figure 2(B).

4.2 | Holling type-II functional response

In this subsection, we consider the following consumer-resource model with Holling type II functional response:

$$\begin{cases} u_t(x, t) = d_{11}u_{xx}(x, t) + u\left(1 - \frac{u}{a}\right) - \frac{buv}{1+u}, & 0 < x < \ell\pi, t > 0, \\ v_t(x, t) = d_{22}v_{xx}(x, t) - d_{21}(v(x, t)u_x(x, t - \tau))_x - cv + \frac{buv}{1+u}, & 0 < x < \ell\pi, t > 0, \\ u_x(0, t) = u_x(\ell\pi, t) = v_x(0, t) = v_x(\ell\pi, t) = 0, & t \geq 0. \end{cases} \quad (50)$$

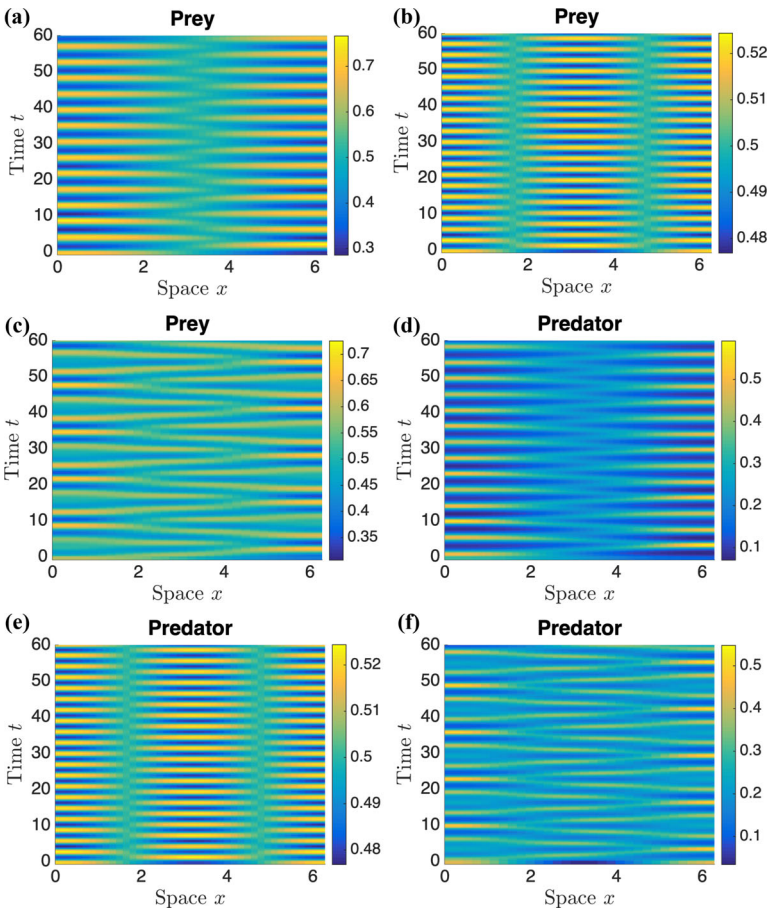


FIGURE 4 Numerical simulations for system (42) with parameters in (45). (A) and (D) $(d_{21}, \tau) = (16.2, 0.85) \in R_1$ in Figure 2(B), convergence to a mode-1 periodic solution with profile $\cos(x/2)$ in space, and the initial conditions are $u(x, 0) = 0.5 + 0.2 \cos(x/2), v(x, 0) = 0.2344 + 0.1 \cos(x/2)$; (B) and (E): $(d_{21}, \tau) = (17.9, 0.728) \in R_2$ in Figure 2(B), convergence to a mode-2 periodic solution with profile $\cos(x)$ in space, and the initial conditions are $u(x, 0) = 0.5 + 0.02 \cos(x), v(x, 0) = 0.2344 + 0.01 \cos(x)$; (C) and (F) $(d_{21}, \tau) = (17, 0.83) \in R_3$ in Figure 2(B), a quasi-periodic spatiotemporal pattern showing the interaction of mode-1 and mode-2 near the double Hopf bifurcation point, and the initial conditions are $u(x, 0) = 0.5 + 0.1 \cos(x/2), v(x, 0) = 0.2344 + 0.2 \cos(x)$

System (50) has a unique positive equilibrium $E_*(\gamma, v_\gamma)$, where

$$\gamma = \frac{c}{b - c}, \quad v_\gamma = \frac{(a - \gamma)(1 + \gamma)}{ab}, \tag{51}$$

provided that $b > \frac{c(1+a)}{a}$ (or equivalently, $0 < \gamma < a$) holds. For this equilibrium $E_*(\gamma, v_\gamma)$, we have

$$a_{11} = \frac{\gamma(a-1-2\gamma)}{a(1+\gamma)} \begin{cases} < 0, & \frac{a-1}{2} < \gamma < a, \\ > 0, & 0 < \gamma < \frac{a-1}{2}, \end{cases} \tag{52}$$

$$a_{12} = -c < 0, \quad a_{21} = \frac{a-\gamma}{a(1+\gamma)} > 0, \quad a_{22} = 0,$$

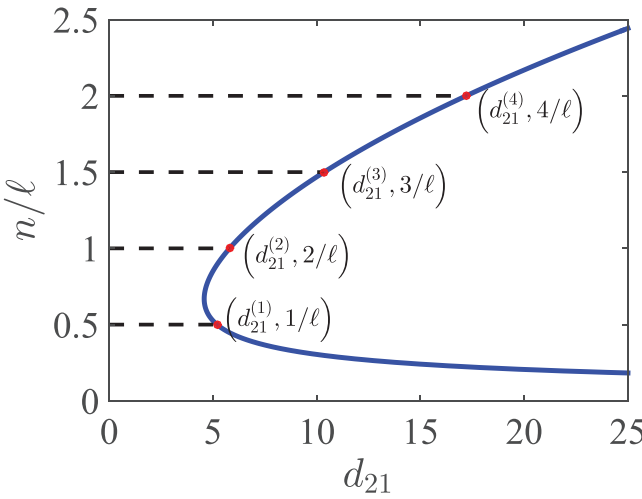


FIGURE 5 The critical values $d_{21}^{(n)}$ with respect to the wave number n for system (50) with parameters in (45). At $d_{21} = d_{21}^{(n)}, Q_n = 0$

and

$$a_{11}^2 + a_{22}^2 + 2a_{12}a_{21} \begin{cases} \geq 0, & c \leq c_*, \\ < 0, & c > c_*, \end{cases} \quad \text{where } c_* = \frac{\gamma^2(a - 1 - 2\gamma)^2}{2a(1 + \gamma)(a - \gamma)}. \tag{53}$$

When $d_{21} = 0$, Hopf and steady-state bifurcations for system (50) with parameter γ have been found in Ref. 28. When $\frac{a-1}{2} < \gamma < a$, we have $a_{11} < 0$ and then $d_{11}a_{22} + d_{22}a_{11} < 0$. Thus, the conditions (C_0) , (C_1) , and (C_2) hold and the positive constant equilibrium $E_*(\gamma, v_\gamma)$ is locally asymptotically stable for any $d_{11}, d_{22} > 0$.

We still use parameters in (45). Then $\gamma = 1, E_*(1, 0.3125), c_* = 0.125$, and $a_{11}^2 + a_{22}^2 + 2a_{12}a_{21} < 0$. So, from By Theorem 3 and Proposition 4, stability switches may occur. From (22) and Proposition 4, we also have $n_* = 2, S_p = \{1\}$. By (25), we can obtain the critical values $d_{21}^{(n)}$ of d_{21} as follows:

$$d_{21}^{(1)} = 5.2 < d_{21}^{(2)} = 5.8 < d_{21}^{(3)} \doteq 10.3556 < d_{21}^{(4)} = 17.2 < \dots \tag{54}$$

Figure 5 shows these critical values for $0 < d_{21} < 25$ and shows that $\min_{n \in \mathbb{N}} d_{21}^{(n)} = d_{21}^{(1)}$. Since $n_* = 2$ and $S_p = \{1\}$, by (26) and (54), we have

$$\min_{n \in S_p} d_{21}^{*(n)} = d_{21}^{*(1)} \doteq 5.0596, \quad \min_{n \notin S_p} d_{21}^{(n)} = d_{21}^{(2)} = 5.8, \tag{55}$$

which, together with (35), implies that

$$d_{21}^* = \min \left\{ \min_{n \in S_p} d_{21}^{*(n)}, \min_{n \notin S_p} d_{21}^{(n)} \right\} = d_{21}^{*(1)} \doteq 5.0596. \tag{56}$$

By (37), we have

$$d_{21}^{**} = \max_{n \in S_p} \left\{ d_{21}^{(n)} \right\} = d_{21}^{(1)} = 5.2. \tag{57}$$

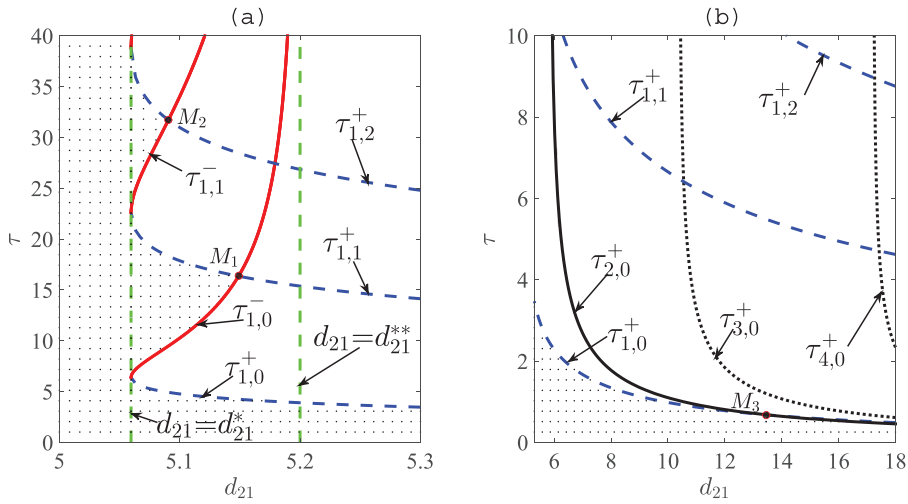


FIGURE 6 Stability region and Hopf bifurcation curves in the d_{21} - τ plane for system (50) with parameters in (45). The dotted region is the stability region and $\tau = \tau_{n,0}^\pm$ is the critical Hopf bifurcation curves for the positive equilibrium $E_*(1, 0.3125)$. (A) Here, the blue dashed curves are the Hopf bifurcation curves $\tau = \tau_{1,j}^+$ with $j = 0, 1, 2$, and the red curves are $\tau = \tau_{1,j}^-$ with $j = 0, 1$; $d_{21} = d_{21}^{**}$ is the vertical asymptotic line of $\tau = \tau_{1,j}^-$, and the Hopf bifurcation curves $\tau = \tau_{1,j}^+$ and $\tau = \tau_{1,j}^-$ are tangent to the vertical line $d_{21} = d_{21}^{**}$. (B) Here, the blue dashed curves are the Hopf bifurcation curves $\tau = \tau_{1,j}^+$ with $j = 0, 1, 2$, and the black curves are $\tau = \tau_{n,0}^+$ with $n = 2, 3, 4$

Thus, according to (30) and Theorem 3, the stability region and Hopf bifurcation curves can be plotted in the d_{21} - τ plane as shown in Figure 6.

For $0 < d_{21} < d_{21}^* \doteq 5.0596$, the positive equilibrium $E_*(1, 0.3125)$ is locally asymptotically stable for any $\tau \geq 0$. For $d_{21}^* < d_{21} < d_{21}^{**} = d_{21}^{(1)} = 5.2$, there exist two sequences of Hopf bifurcation values $\{\tau_{1,j}^+\}$ and $\{\tau_{1,j}^-\}$. The alternating occurrence of the two sequences of Hopf bifurcation values leads to a delay-induced stability switches when increasing the delay value τ (see Figure 6(A)). The Hopf bifurcation curves $\tau = \tau_{1,0}^-$ and $\tau = \tau_{1,1}^+$ interact at the point $M_1(5.1488, 16.3545)$, and Hopf bifurcation curves $\tau = \tau_{1,1}^-$ and $\tau = \tau_{1,2}^+$ interact at the point $M_2(5.0906, 32)$. For fixed $d_{21} = 5.12 \in (d_{21}^*, d_{21}^{**})$, from (30), we have a sequence of Hopf bifurcation values as follows:

$$\tau_{1,0}^+ \doteq 4.5183 < \tau_{1,0}^- \doteq 12.1765 < \tau_{1,1}^+ \doteq 17.1357 < \tau_{1,2}^+ \doteq 29.7532 < \tau_{1,1}^- \doteq 39.7247. \tag{58}$$

From Lemma 1, the positive constant equilibrium E^* is locally asymptotically stable for $\tau \in (0, \tau_{1,0}^+) \cup (\tau_{1,0}^-, \tau_{1,1}^+)$, and is unstable for $\tau \in (\tau_{1,0}^+, \tau_{1,0}^-) \cup (\tau_{1,1}^+, +\infty)$. Figure 7 shows the changes of the asymptotic spatiotemporal patterns for system (50) with the increase of the delay τ . For $\tau = 4 < \tau_{1,0}^+$, the positive equilibrium E_* is locally asymptotically stable, as shown in Figures 7(A) and (E); for $\tau = 4.6 \in (\tau_{1,0}^+, \tau_{1,0}^-)$, E_* is unstable and a mode-1 periodic solution with spatial profile $\cos(x)$ appears as the result of Hopf bifurcation at $\tau = \tau_{1,0}^+$, as shown in Figures 7(B) and (F); for $\tau = 14 \in (\tau_{1,0}^-, \tau_{1,1}^+)$, the positive equilibrium E_* regains the stability, as shown in Figures 7(C) and (G); and for $\tau = 17.16 > \tau_{1,1}^+$, the positive equilibrium E_* becomes unstable again and a mode-1 periodic solution with spatial profile $\cos(x)$ appears again, as shown in Figures 7(D) and (H).

For $d_{21} \geq d_{21}^{**}$, there exist Hopf bifurcation values like $\tau_{n,j}^+$ and no Hopf bifurcation values like $\tau_{n,j}^-$, and there exists a positive bifurcation value τ_* such that the positive equilibrium $E_*(1, 0.3125)$ is locally asymptotically stable for $\tau < \tau_*$ and unstable for $\tau > \tau_*$. Figure 6(B) shows these Hopf

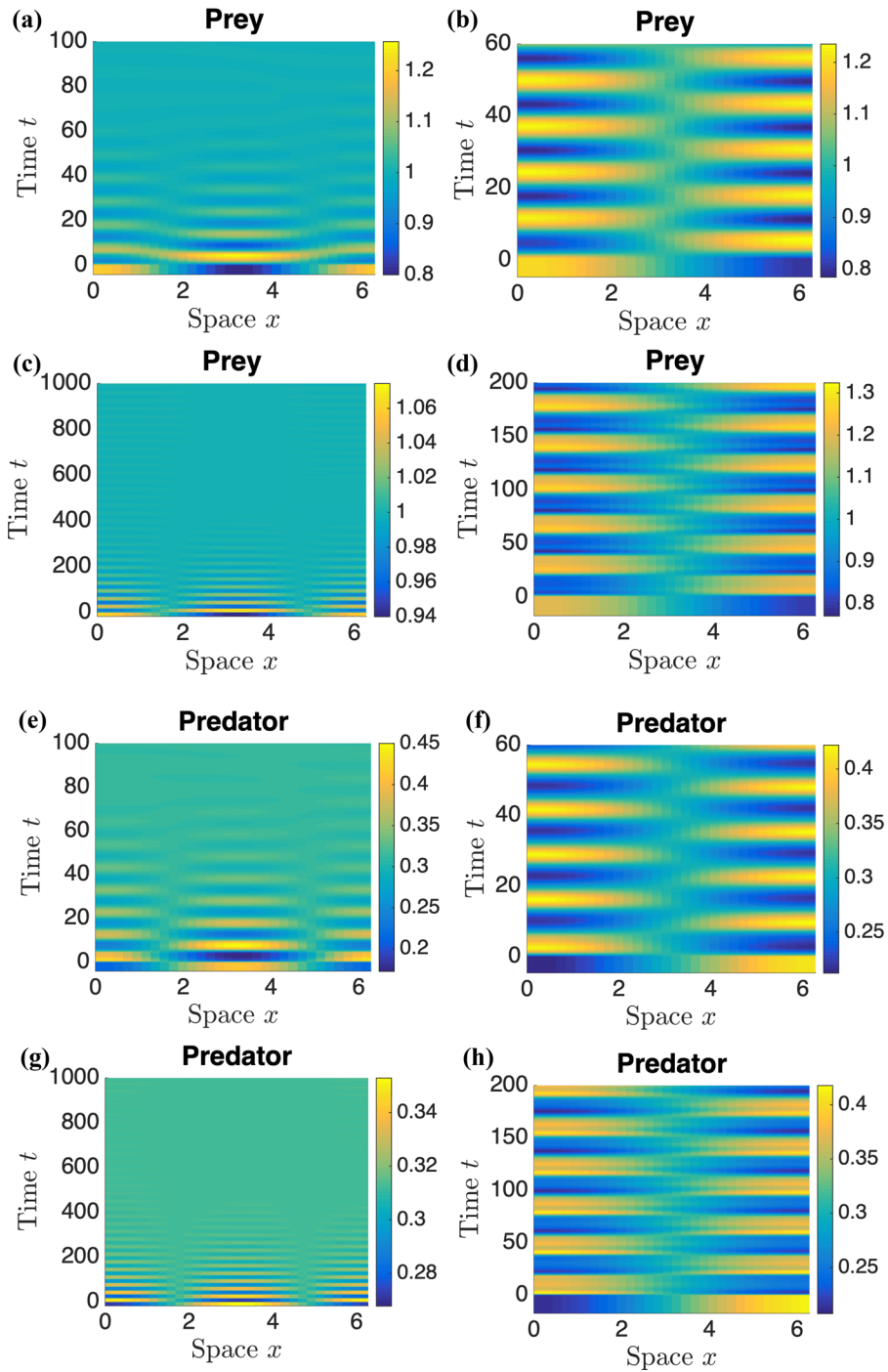


FIGURE 7 Numerical simulations for system (50) with parameters in (45) and $d_{21} = 5.12$. (A) and (E) $\tau = 4 < \tau_{10}^+$; (B) and (F) $\tau = 4.6 \in (\tau_{1,0}^+, \tau_{1,0}^-)$; (C) and (G): $\tau = 14 \in (\tau_{1,0}^-, \tau_{1,0}^+)$; (D) and (H) $\tau = 17.16 > \tau_{1,1}^+$. The initial conditions are chosen as $u(x, 0) = 1 + 0.2 \cos(x)$, $v(x, 0) = 0.3125 - 0.1 \cos(x)$ except for (C) and (G), and the initial conditions for (C) and (G) are $u(x, 0) = 1 + 0.06 \cos(x)$, $v(x, 0) = 0.3125 - 0.04 \cos(x)$

bifurcation curves for $5.3 \leq d_{21} \leq 18, 0 \leq \tau \leq 10$. The Hopf bifurcation curves $\tau = \tau_{1,0}^-$ and $\tau = \tau_{2,0}^+$ interact at the point $M_3(13.4531, 0.6811)$ and it is shown that $\tau_* = \tau_{1,0}^+$ for $d_{21}^{**} \leq d_{21} < 13.4531$ and $\tau_* = \tau_{2,0}^+$ for $13.4531 < d_{21} \leq 18$.

5 | DISCUSSION

In this paper, we apply the derivation of the single-species spatial memory model originally proposed by Shi et al⁵ to model the consumer-resource interaction with consumer's spatial memory. This novel model has broad applicability in better describing consumer-resource interactions than nonspatial memory models because the spatial memory of any consumer naturally exists and is especially pivotal for species with long life span and long-term memory, such as blue whales.^{3,4} The movement of blue whales shows similar dynamical behaviors of our model, and the corresponding author is collaborating with Bill Fagan on this direction that requires massive datasets and parametrization. Under the assumption that the coexistence equilibrium of the system without memory-based diffusion is asymptotically stable, we investigate the effects of the memory-based diffusion coefficient d_{21} and the averaged memory period τ of the consumer on stability. We show that the consumer's memory-based diffusion has significant influence on stability and generates rich dynamics.

We summarize the effects of the memory-based diffusion coefficient and the averaged memory period of the consumer on stability as follows: (i) When d_{21} is small enough ($d_{21} < d_{21}^*$), the delay τ does not affect stability, that is, the coexistence equilibrium is always stable for any $\tau \geq 0$. (ii) When d_{21} is moderate ($d_{21}^* < d_{21} < d_{21}^{**}$), there are two kinds of critical values $\tau_{n,j}^+$ and $\tau_{n,j}^-$ of Hopf bifurcations and the delay τ may induce stability switches. (iii) When d_{21} is large enough ($d_{21} > d_{21}^{**}$), only one kind of the critical values $\tau_{n,j}^+$ of Hopf bifurcations exists, and the coexistence equilibrium is stable for τ less than some critical value and unstable for τ larger than this critical value.

The impact of spatial memory on the consumer-resource dynamics is different from the impact in the single-species model,⁵ where the stability of the coexistence equilibrium is independent of the time delay and no delay-induced Hopf bifurcation occurs. However, for the consumer-resource model with random and memory-based diffusions, delay-induced Hopf bifurcation and double Hopf bifurcation can occur. This phenomenon is partially similar to the model that incorporates the maturation delay into the single-species spatial memory model.⁷ For the Holling type-I functional response, when $d_{21}^* < d_{21} < d_{21}^{**}$, there are delay-induced Hopf bifurcation and double Hopf bifurcation but no stability switches. This double Hopf bifurcation is generated by the interaction of Hopf bifurcations with different wave numbers. However, for the Holling type-II functional response, when $d_{21}^* < d_{21} < d_{21}^{**}$, there exist delay-induced stability switches and double Hopf bifurcation, which is generated by the interaction of Hopf bifurcations with the same wave number.

If we start with a random diffusion model without Turing bifurcation to incorporate spatial memory, then Turing bifurcation cannot be induced by spatial memory. If we incorporate spatial memory into a random diffusion model with Turing instability, how does spatial memory regulate Turing patterns? This is an open question for future study. For instance, when the functional response is chosen as the ratio-dependent type where Turing bifurcation and Turing-Hopf bifurcation exist,²⁹ we conjecture that spatial memory can result in much more complicated dynamics.

This paper formulates and studies a diffusive consumer-resource model with explicit spatial memory of the consumer because the producer naturally has no memory or cognition. It is an intriguing problem to study a diffusive prey-predator model with spatial memory/cognition in both prey and predators, where prey are small animals instead of plants. In this case, rigorous mathematical analysis will be extremely challenging, and new mathematical techniques are expected to be developed.

ACKNOWLEDGMENTS

We would like to thank the editor and reviewers for their valuable comments and suggestions, which significantly improve the quality of our paper.

This work was partially supported by grants from National Natural Science Foundation of China (No.11971143 and 12071105), Zhejiang Provincial Natural Science Foundation of China (No.LY19A010010), National Science Foundation of United States (DMS-1715651), and Natural Sciences and Engineering Research Council of Canada (Discovery Grant RGPIN-2020-03911 and Accelerator Grant RGPAS-2020-00090).

ORCID

Junping Shi  <https://orcid.org/0000-0003-2521-9378>

Hao Wang  <https://orcid.org/0000-0002-4132-6109>

REFERENCES

1. Fagan WF, Lewis MA, Auger-Methe M, et al. Spatial memory and animal movement. *Ecol Lett.* 2013;16(10):1316-1329.
2. Salmani Y, Thompson P, Wang H, Wang X, Marley J, Lewis M. Memory and learning in animal movement models. Preprint. 2021.
3. Abrahms B, Hazen EL, Aikens EO, et al. Memory and resource tracking drive blue whale migrations. *Proc Natl Acad Sci USA.* 2019;116(12):5582-5587.
4. Fagan WF. Migrating whales depend on memory to exploit reliable resources. *Proc Natl Acad Sci USA.* 2019;116(12):5217-5219.
5. Shi J, Wang C, Wang H, Yan X. Diffusive spatial movement with memory. *J Dyn Differ Equ.* 2020;32(2):979-1002.
6. An Q, Wang C, Wang H. Analysis of a spatial memory model with nonlocal maturation delay and hostile boundary condition. *Discrete Contin Dyn Syst.* 2020;40(10):5845-5868.
7. Shi J, Wang C, Wang H. Diffusive spatial movement with memory and maturation delays. *Nonlinearity.* 2019;32(9):3188-3208.
8. Shi Q, Shi J, Wang H. Spatial movement with distributed memory. *J Math Biol.* 2021;82(4):33.
9. Song Y, Wu S, Wang H. Spatiotemporal dynamics in the single population model with memory-based diffusion and nonlocal effect. *J Differ Equ.* 2019;267(11):6316-6351.
10. Song Y, Wu S, Wang H. Memory-based movement with spatiotemporal distributed delays in diffusion and reaction. *Appl Math Comput.* 2021;404:126254.
11. Fagan WF, Gurarie E, Bewick S, Howard A, Cantrell RS, Cosner C. Perceptual ranges, information gathering, and foraging success in dynamic landscapes. *Am Nat.* 2017;189(5):474-489.
12. Cosner C. Reaction-diffusion-advection models for the effects and evolution of dispersal. *Discrete Contin Dyn Syst.* 2014;34(5):1701-1745.
13. Wang J, Wu S, Shi J. Pattern formation in diffusive predator-prey systems with predator-taxis and prey-taxis. *Discrete Contin Dyn Syst Ser B.* 2021;26(3):1273-1289.
14. Ainseba B, Bendahmane M, Noussair A. A reaction-diffusion system modeling predator-prey with prey-taxis. *Nonlinear Anal Real World Appl.* 2008;9(5):2086-2105.
15. Kareiva P, Odell GT. Swarms of predators exhibit "preytaxis" if individual predators use area-restricted search. *Am Nat.* 1987;130:233-270.

16. Lee JM, Hillen T, Lewis MA. Continuous traveling waves for prey-taxis. *Bull Math Biol.* 2008;70(3):654-676.
17. Lee JM, Hillen T, Lewis MA. Pattern formation in prey-taxis systems. *J Biol Dyn.* 2009;3(6):551-573.
18. Jin H-Y, Wang Z-A. Global stability of prey-taxis systems. *J Differ Equ.* 2017;262(3):1257-1290.
19. Liu P, Shi J, Wang Z-A. Pattern formation of the attraction-repulsion Keller-Segel system. *Discrete Contin Dyn Syst Ser B.* 2013;18(10):2597-2625.
20. Tao Y. Global existence of classical solutions to a predator-prey model with nonlinear prey-taxis. *Nonlinear Anal Real World Appl.* 2010;11(3):2056-2064.
21. Wang Q, Song Y, Shao L. Nonconstant positive steady states and pattern formation of 1D prey-taxis systems. *J Nonlinear Sci.* 2017;27(1):71-97.
22. Wang X, Wang W, Zhang G. Global bifurcation of solutions for a predator-prey model with prey-taxis. *Math Methods Appl Sci.* 2015;38(3):431-443.
23. Wu S, Shi J, Wu B. Global existence of solutions and uniform persistence of a diffusive predator-prey model with prey-taxis. *J Differ Equ.* 2016;260(7):5847-5874.
24. Xiang T. Global dynamics for a diffusive predator-prey model with prey-taxis and classical Lotka-Volterra kinetics. *Nonlinear Anal Real World Appl.* 2018;39:278-299.
25. Wu S, Wang J, Shi J. Dynamics and pattern formation of a diffusive predator-prey model with predator-taxis. *Math Models Methods Appl Sci.* 2018;28(11):2275-2312.
26. Lunardi A. *Analytic Semigroups and Optimal Regularity in Parabolic Problems*, Volume 16 of Progress in Nonlinear Differential Equations and Their Applications. Birkhäuser Verlag; 1995.
27. Murray JD. *Mathematical Biology. II: Spatial Models and Biomedical Applications*, Volume 18 of Interdisciplinary Applied Mathematics. 3rd ed. Springer-Verlag; 2003.
28. Yi F, Wei J, Shi J. Bifurcation and spatiotemporal patterns in a homogeneous diffusive predator-prey system. *J Differ Equ.* 2009;246(5):1944-1977.
29. Song Y, Zou X. Bifurcation analysis of a diffusive ratio-dependent predator-prey model. *Nonlinear Dyn.* 2014;78(1):49-70.

How to cite this article: Song Y, Shi J, Wang H. Spatiotemporal dynamics of a diffusive consumer-resource model with explicit spatial memory. *Stud Appl Math.* 2022;148:373–395. <https://doi.org/10.1111/sapm.12443>